Electronic Supplementary Material (ESI) for Nanoscale.

Supporting Information: Impact of invasive metal probes on Hall measurements in semiconductor nanostructures

Jan G. Gluschke,[a] Jakob Seidl,[a] H. Hoe Tan,[b] Chennupati Jagadish,[b] Philippe Caroff [b,c] and Adam P. Micolich *[a]

[a] School of Physics, University of New South Wales, Sydney NSW 2052, Australia
[b] Department of Electronic Materials Engineering, Research School of Physics, The Australian National University, Canberra, ACT 2601, Australia
[c] Microsoft Quantum Lab Delft, Delft University of Technology, 2600 GA Delft, The Netherlands

*E-mail: adam.micolich@nanoelectronics.physics.unsw.edu.au

Extension of invasive probes down the side facets of the nanostructure.

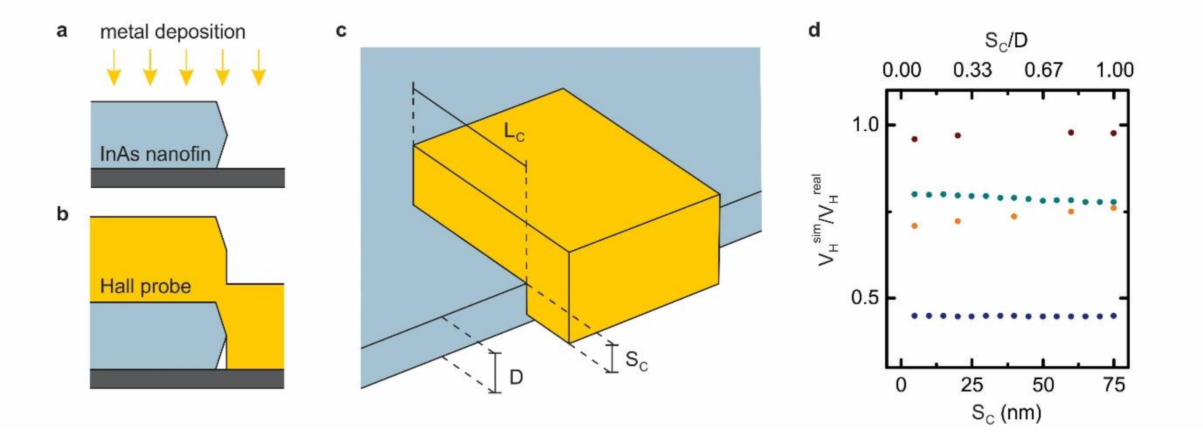

Figure S1. (a) Illustration of metal deposition on an InAs nanofin with angled side facets (cross-sectional view, not to scale). (b) Only the top side facet is contacted due to the directionality of the metal deposition by thermal evaporation. (c) Illustration of the model of a Hall probe with an overlap of the probe and nanofin side S_C. (d) Simulated Hall voltage V_H^{sim} for different contact geometries on a 75 nm thick nanofin. All contacts are 300 nm wide. The modelled probes for the different colours are: (blue) L_C = 300 nm, no contact resistance, (cyan) L_C = 50 nm, no contact resistance, (orange) L_C = 300 nm, high contact resistance σ_{CR} = 10 S/m, (red) L_C = 50 nm, high contact resistance σ_{CR} = 10 S/m.

The metal probes deposited on the nanofin need to step down from the top facet of the nanostructure to the substrate. The probe may consequently cover part of the side of the nanofin. This side coverage S_C can, in principle, vary between 0 and 100%, depending on metal deposition method and the geometry of the nanostructure side facets. In our case, we used a side coverage of 50%. This is because the side wall of InAs nanofins consists of two side facets as illustrated in Figure S1a.[1] The top facet will likely mask the bottom facet during metal deposition leading to the metal probe only contacting the top half of the side wall (see Figure S1b). Regardless, we conducted simulations to find that the side coverage does not significantly impact the Hall voltage measurements. Figure S1d shows the simulated Hall voltage V_H^{sim} for different degrees of coverage. The changes in V_H^{sim} are small. There is virtually no change for the blue data points, which represent a typical probe geometry. The probe pairs with high contact resistance show a slight increase in V_H^{sim} as a function of S_C. This is because the electrical potential on the side surface is equal to or larger than that probed at any point on the top surface. The overall measured potential is therefore higher. The opposite dependence is observed for the short contact without contact resistance (cyan). Here, the side coverage adds to the current perturbation effect reducing V_H^{sim}. The effect of probe coverage of side facets will be more relevant for taller narrower nanostructures such as nanowires.

Recessed Hall probes – Nanoscale Hall bars and nanocross structures

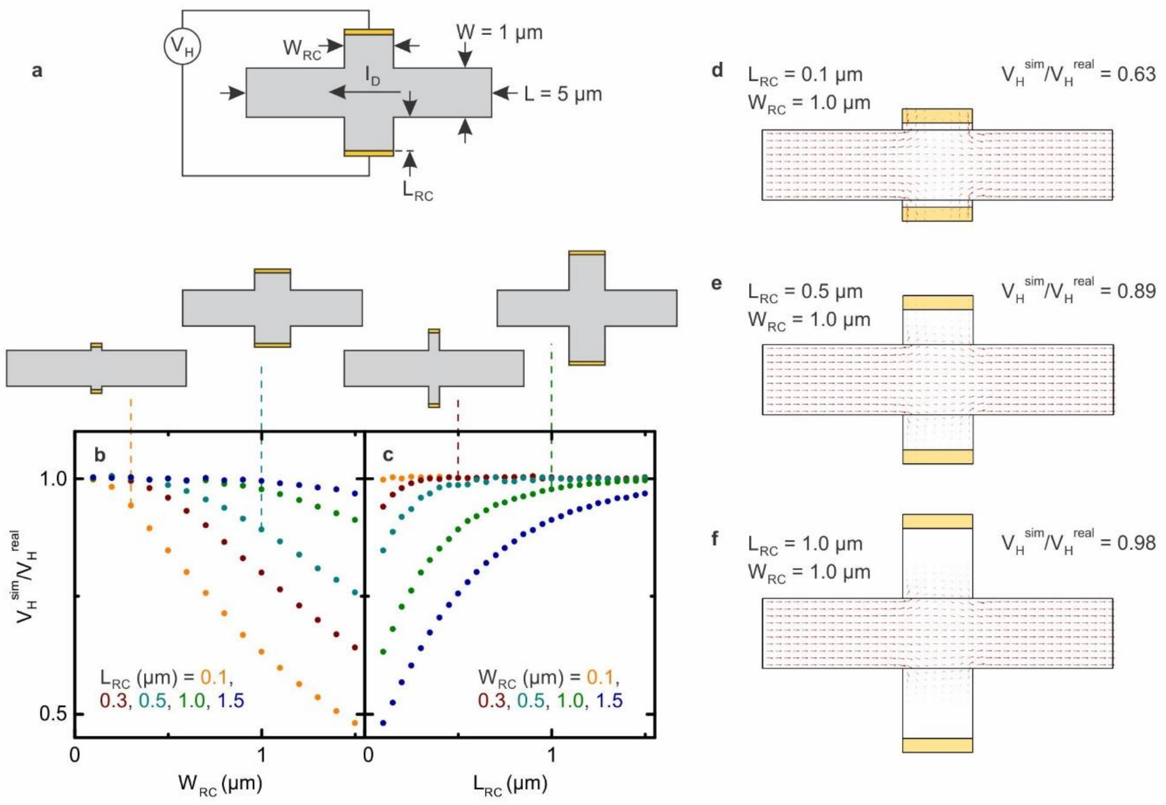

Figure S2. (a) Schematic of a nanoscale Hall bar with recessed contacts width W_{RC} and length L_{RC}. (b) V_H^{sim}/V_H^{real} vs W_{RC} for different L_{RC}. (c) V_H^{sim}/V_H^{real} vs L_{RC} for different W_{RC}. Modelled current density in a device with (d) 0.1 µm, (e) 0.5 µm, and (f) 1.0 µm long recessed contacts.

Ideal Hall bars have high aspect ratio L/W and recessed Hall probes with probe widths $W_{RC} << W$ and probe lengths $L_{RC} >> W_{RC}$. Some 2D nanoscale devices such as nanocrosses[2,3] have recessed probes but the conditions outlined above are not always fulfilled. Figure S2b shows V_H^{sim}/V_H^{real} vs W_{RC} for a range of L_{RC}. The channel dimensions are L = 5 µm and W = 1 µm for all simulations. V_H^{sim}/V_H^{real} decreases as W_{RC} increases. This effect is more pronounced for shorter probes. Accordingly, Figure S2c shows that V_H^{sim}/V_H^{real} decreases as L_{RC} decreases with W_{RC} held constant.

The reduction in V_H^{sim}/V_H^{real} can be attributed to the current-perturbation effect discussed in Section 3.4 of the main text. The metal contacts provide an alternative a path of lower resistance through the probed semiconductor segment, when L_{RC} is approximately equal to or smaller than W_{RC}. If, in addition, W_{RC} is of the order of L and W, the current density and electrical potential profile in the semiconductor channel is significantly distorted. This leads to a reduced (simulated) probed Hall voltage. The distortion of current density due to recessed contacts is illustrated in Figure S2d-f. The current density in the channel is decreased significantly for the 0.1 µm long contact in Figure S2d, leading to a reduction in V_H^{sim} by 37% relative to V_H^{real}. The longer contacts shown in Figure S2e,f are nearly non-invasive. They cause less current perturbation, resulting in higher V_H^{sim}/V_H^{real}.

Based on our simulations, we recommend that devices with recessed contacts are designed, where possible, so that $W_{RC} < L/3$, $W_{RC} < W$, $W_{RC} < L_C$, $W < L/3$. Under these conditions V_H^{sim} is no less than 5% lower than V_H^{real}. For $W_{RC} < 2L_{RC}$, V_H^{sim} is no less than 11% lower than V_H^{real}.

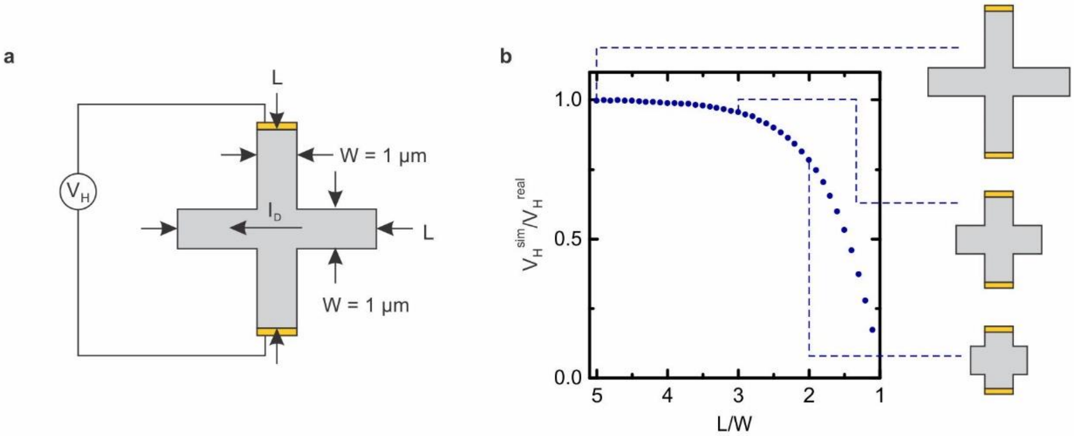

Figure S3. (a) Equilateral nanocross geometry for Hall measurements. (b) V_H^{sim}/V_H^{real} for different device length to contact width ratios L/W. All simulations use W = 1 μm.

Some nanodevices have an equilateral cross geometry[3] as shown in Figure S3a. We performed simulations for different equilateral cross geometries to estimate the reduction in Hall voltage due to current perturbation and geometrical effects. Figure S3b shows V_H^{sim}/V_H^{real} for different L/W ratios. For such devices, $V_H^{sim}/V_H^{real} > 0.97$ for $L/W > 5$. Even for $L/W > 3$, the recessed probes remain relatively non-invasive giving $V_H^{sim}/V_H^{real} > 0.95$. As L/W approaches 2, we see a significantly increasing reduction in V_H^{sim}/V_H^{real}.

Impact of multiple probe pairs on Hall voltage measurements

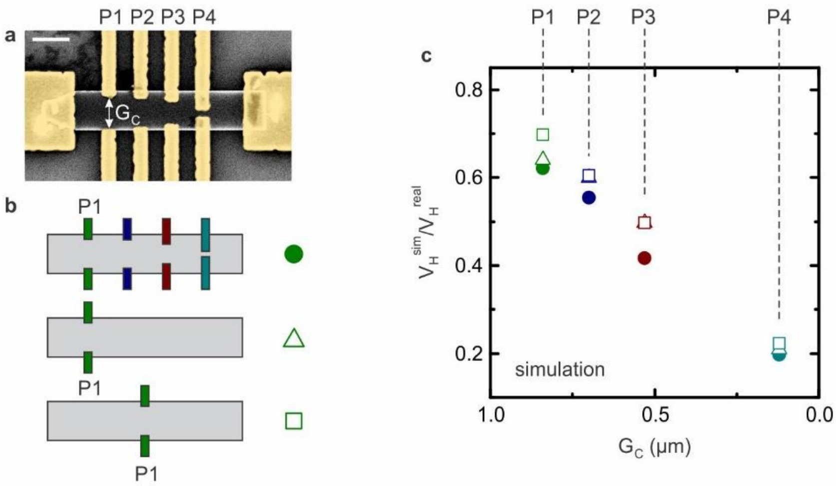

Figure S4. (a) Device with four probe pairs P1-P4. (b) Schematic of the model used in simulation. (c) Hall voltage V_H^{sim} was simulated in three different configurations for each probe pair: probe pair in complete device (circle), probe pair in original position with all other probes removed (triangle), probe pair in centre of the channel with all other probes removed (square).

Characterizing Hall probes on the same nanofin eliminates sample-to-sample variations. This is important for the study of the effects of probe geometry because carrier concentrations can vary between nanofins (see Section 3.6 in the main text). Figure S4a shows a device with four probe pairs with different probe separations G_C designed to study the effect of Hall probe length. It stands to reason that the measured Hall voltage is not only impacted by G_C but also by: (i) the positioning of the Hall probe relative to source and drain contacts (see Section 3.3 in the main text), as well as (ii) current perturbation from adjacent Hall probes. Both effects should reduce the probed Hall voltage.

We performed a set of simulations to estimate the impact of (i) and (ii) on Hall voltage measurements using the example of the device shown with four probe pairs P1-P4. This is the same device as shown in Figure 2a of the main text. V_H^{sim} was simulated for each probe pair in the three geometries shown in Figure S4b: (solid circle) in the complete device with all probes, (open triangle) probe pair in the same position without other probes, and (open square) without other probes at the centre of the samples. Figure S4c shows V_H^{sim}/V_H^{real} vs G_C for the three configurations. P3 is most impacted by the removal of other contacts because it is adjacent to P4 which has the largest overlap with the nanofin causing a significant perturbation to the electrical potential. P1 and P4 show the largest relative increase in V_H^{sim} between the configurations indicated by the open triangle and open square because their original position was closest to the source and drain contacts. Overall, the differences between device geometries (solid circle/open triangle/open square) are small relative to the trend of V_H^{sim}/V_H^{real} vs G_C. Regardless, the effect of (i) and (ii) should be considered when designing and evaluating data from Hall devices. Only a single pair of Hall probes should be used at the centre of the sample where possible. In the case of this work, all simulations relating to real devices were modelled with all contact pairs. This means that the effects associated with the use of multiple probe pairs are taken into account.

Table of reduction in Hall voltage for different sample and contact geometries

Table ST1 shows the simulated Hall voltage V_H^{sim} compared to the real Hall voltage V_H^{real} as defined in the main text. The modelled nanofin width W was 1 µm. The model was computed for nanofin lengths L of 1 µm and 2 µm and thicknesses D of 10 nm and 100 nm with various probe dimensions at a magnetic field B = 0.1 T. All models are for a single Hall probe pair at the centre of the sample without contact resistance. Figure S5 shows the current density for two device geometries.

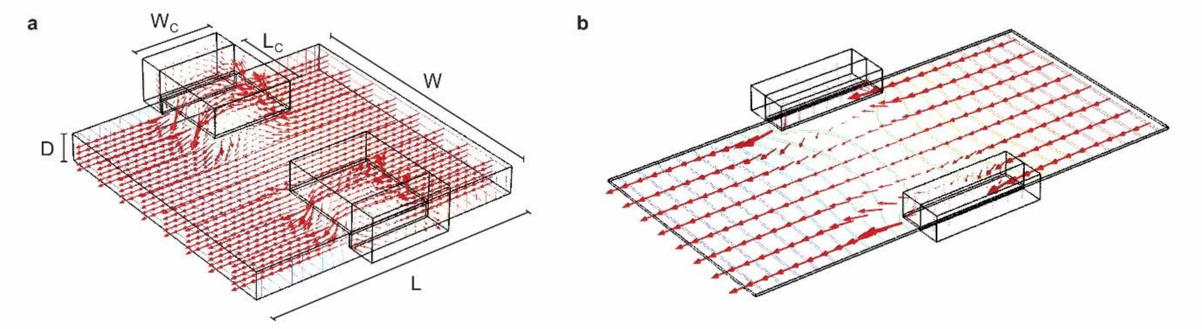

Figure S5. (a) Model of current density through a nanofin device with thickness D = 100 nm, length L = 1 µm, width W = 1 µm, contact length L_C = 0.3 µm, contact width W_C = 0.3 µm. (b) Model of current density through a nanofin dimensions D = 10 nm, L = 2 µm, W = 1 µm, L_C = 0.1 µm, W_C = 0.5 µm.

Table ST1. V_H/V_H^{real} for different geometries.

D/W	L/W	L_C/W	W_C/W	V_H/V_H^{real}
0.1	1	0.01	0.01	0.67
0.1	1	0.01	0.05	0.65
0.1	1	0.01	0.1	0.62
0.1	1	0.01	0.3	0.50
0.1	1	0.01	0.5	0.37
0.1	1	0.05	0.01	0.64
0.1	1	0.05	0.05	0.62
0.1	1	0.05	0.1	0.59
0.1	1	0.05	0.3	0.46
0.1	1	0.05	0.5	0.34
0.1	1	0.1	0.01	0.59
0.1	1	0.1	0.05	0.57
0.1	1	0.1	0.1	0.54
0.1	1	0.1	0.3	0.41
0.1	1	0.1	0.5	0.28
0.1	1	0.3	0.01	0.41
0.1	1	0.3	0.05	0.38
0.1	1	0.3	0.1	0.35
0.1	1	0.3	0.3	0.23
0.1	1	0.3	0.5	0.13
0.1	2	0.01	0.01	0.92
0.1	2	0.01	0.05	0.90
0.1	2	0.01	0.1	0.88
0.1	2	0.01	0.3	0.77
0.1	2	0.01	0.5	0.65
0.1	2	0.05	0.01	0.89
0.1	2	0.05	0.05	0.87
0.1	2	0.05	0.1	0.85
0.1	2	0.05	0.3	0.73
0.1	2	0.05	0.5	0.61
0.1	2	0.1	0.01	0.84
0.1	2	0.1	0.05	0.82
0.1	2	0.1	0.1	0.79
0.1	2	0.1	0.3	0.66
0.1	2	0.1	0.5	0.55
0.1	2	0.3	0.01	0.62
0.1	2	0.3	0.05	0.59
0.1	2	0.3	0.1	0.55
0.1	2	0.3	0.3	0.41
0.1	2	0.3	0.5	0.32

D/W	L/W	L_C/W	W_C/W	V_H/V_H^{real}
0.01	1	0.01	0.01	0.66
0.01	1	0.01	0.05	0.63
0.01	1	0.01	0.1	0.60
0.01	1	0.01	0.3	0.46
0.01	1	0.01	0.5	0.33
0.01	1	0.05	0.01	0.61
0.01	1	0.05	0.05	0.58
0.01	1	0.05	0.1	0.54
0.01	1	0.05	0.3	0.39
0.01	1	0.05	0.5	0.27
0.01	1	0.1	0.01	0.55
0.01	1	0.1	0.05	0.52
0.01	1	0.1	0.1	0.47
0.01	1	0.1	0.3	0.33
0.01	1	0.1	0.5	0.21
0.01	1	0.3	0.01	0.36
0.01	1	0.3	0.05	0.32
0.01	1	0.3	0.1	0.28
0.01	1	0.3	0.3	0.17
0.01	1	0.3	0.5	0.09
0.01	2	0.01	0.01	0.92
0.01	2	0.01	0.05	0.89
0.01	2	0.01	0.1	0.86
0.01	2	0.01	0.3	0.73
0.01	2	0.01	0.5	0.61
0.01	2	0.05	0.01	0.86
0.01	2	0.05	0.05	0.83
0.01	2	0.05	0.1	0.78
0.01	2	0.05	0.3	0.66
0.01	2	0.05	0.5	0.54
0.01	2	0.1	0.01	0.80
0.01	2	0.1	0.05	0.76
0.01	2	0.1	0.1	0.72
0.01	2	0.1	0.3	0.58
0.01	2	0.1	0.5	0.47
0.01	2	0.3	0.01	0.55
0.01	2	0.3	0.05	0.51
0.01	2	0.3	0.1	0.46
0.01	2	0.3	0.3	0.33
0.01	2	0.3	0.5	0.25

References

1 J. Seidl, J. G. Gluschke, X. Yuan, S. Naureen, N. Shahid, H. H. Tan, C. Jagadish, A. P. Micolich and P. Caroff, *Nano Lett.*, 2019, **19**, 4666–4677.

2 H. Schmid, M. Borg, K. Moselund, L. Cignac, C. M. Breslin, J. Bruley, D. Cutaia and H. Riel, *Appl. Phys. Lett.*, 2015, **106**, 233101.

3 J. Gooth, M. Borg, H. Schmid, V. Schaller, S. Wirths, K. Moselund, M. Luisier, S. Karg and H. Riel, *Nano Lett.*, 2017, **17**, 2596–2602.